scientific reports

Check for updates

OPEN

Insights into the special physiology of *Mortierella alpina* cultured by agar supported solid state fermentation in enhancing arachidonic acid enriched lipid production

Tingting Liu[1,2,3,4], Pandeng Li[1,2,4], Ziqi Ou[1], Yumei Feng[1,2,3], Bohan Wang[1,2,3], Tianyi Yu[1,2], Yuanmin Zhu[1,2,3]✉ & Longjiang Yu[1,2,3]✉

Solid-state fermentation (SSF), an eco-friendly technology, has shown the high-yield ability to produce products such as biodiesel, pharmaceuticals, and enzymes. However, it has not yet demonstrated an advantage in ARA-containing lipids production. This study demonstrated that agar-supported SSF (AgSF) could induce *Mortierella alpina* M0223 to yield higher ARA-rich lipids than submerged fermentation (SmF), and elucidated the underlying mechanisms by the comparative transcriptome. AgSF-M0223 formed a mycelial network consisting mainly of surface (SH) and aerial hyphae (AH). The attenuated citrate cycle of SH compared to SmF was coupled with enhanced triglyceride biosynthesis, glycerophospholipid metabolism, and underlying increases in NADPH supply, prompting more glucose flux towards ARA-rich lipid synthesis. Besides, AH has high initial lipid and ARA amounts, while its primary metabolism was weakened due to nutrient scarcity, demonstrating attenuated lipid synthesis. The unique ARA and lipid synthesis characteristics of SH and AH enabled AgSF-M0223 to achieve high-yield ARA-rich lipids. By supplementing nutrients to AH through a spraying strategy and optimizing nutrients for SH, lipid yields reached 12.64 g/L comprising 70.41% ARA, 1.63 times higher than before optimization. These findings provided new insights into fungal physiology under SSF, and presented a promising eco-friendly paradigm for ARA production with advances in mechanical automation.

Keywords *Mortierella alpina*, Arachidonic acid, Lipid, Agar-supported solid-state fermentation, Surface hyphae

Polyunsaturated fatty acids (PUFAs), innate structural components of cell membranes, play an important role in membrane physical properties[1]. Arachidonic acid (ARA), the most abundant C20 PUFA in humans, can act as precursors of endogenous cannabinoid or eicosanoids involved in a variety of cellular processes, such as inflammation, mood, cognitive functions improvement and central nervous system development[2]. Accordingly, ARA has been widely used in pharmaceuticals, nutrition, cosmetics, breeding feed and other fields[3]. Lipids of microbial sources have been suggested as the main alternative source of ARA[4]. Submerged fermentation (SmF) of *Mortierella alpina* (*M. alpina*) is the main way to produce ARA[5].

In recent years, solid-state fermentation (SSF) has emerged as a promising alternative to SmF due to its advantages, including reduced wastewater production, lower energy consumption, and higher productivity. SSF is a biotechnological process in which microorganism are cultivated in environments with little or no free water,

[1]Department of Biotechnology, College of Life Science and Technology, Institute of Resource Biology and Biotechnology, Huazhong University of Science and Technology, Wuhan 430074, China. [2]Key Laboratory of Molecular Biophysics, Ministry of Education, Huazhong University of Science and Technology, Wuhan 430074, China. [3]Hubei Food and Medicine Resources Engineering Research Center, Huazhong University of Science and Technology, Wuhan 430074, China. [4]Tingting Liu and Pandeng Li contributed equally to this work. ✉email: zhuyuanmin@hust.edu.cn; yulongjiang@hust.edu.cn

which mimics the natural habitat of fungi, particularly filamentous fungi, thereby enhancing product yield. Enzyme production is one of the most successful applications of microbial SSF, with the production of various enzymes, including cellulase, amylase, protease, and xylanase, successfully achieved through SSF of filamentous fungi[6]. Furthermore, the high productivity of SSF has facilitated its application in biofuel production, such as the synthesis of lipase by *Rhizopus oligosporus*[7] for biodiesel catalysis, and the ability of fungi like *Mucor indicus* and *Rhizopus oryzae* to produce ethanol, with a yield of up to 74% of the theoretical maximum[8]. Additionally, SSF is frequently employed in the production of bioactive compounds[9], such as phenolic compounds, and in the enhancement of plant-derived proteins[10]. Thus, SSF has established credibility in the production of a broad range of products, including biodiesel, feed bioproducts[11], enzyme, bioactive compounds and polyunsaturated fatty acids (PUFAs).

Zygomycetes possess the ability to synthesize lipids that contain a wide range of polyunsaturated fatty acids, which are commonly used in PUFA[12] production and have been successfully applied in solid-state fermentations (SSFs). *Mucor circinelloides*, a strain known for producing gamma-linolenic acid (GLA), generated 42.43 mg of lipids per gram of dry substrate, with a high proportion of unsaturated fatty acids, when utilizing mulberry branches as a solid substrate[13]. Similarly, *Mortierella isabellina* can produce 47.9 mg lipid per gram of soybean hull, representing a 3.3-fold increase in lipid content compared to the initial lipid content of the soybean hulls[14]. Currently, the SSF of Zygomycetes fungus *M. alpina* primarily focuses on the utilization of natural substrates such as agro-industrial and food by-products including oat bran[15], oilseed cakes[16], grains[17], animal fat by-products[18], and mushrooms[19], yielding lipids with 30–50% ARA and 15–40 mg of ARA per gram of substrate. Although natural substrate is a cost-effective solid matrix, the ARA content and lipid yield remain insufficient to meet the quality and yield for ARA-related products. Furthermore, separating mycelium from the natural biomass matrix is challenging, which hinders the analysis of the mycelium's characteristics, lipid and ARA production capacity, and physiological status[20]. This complicates the understanding of the mechanisms involved in the SSF of *M. alpina*. Agar-supported solid-state fermentation (AgSF) is commonly used for the isolation, preservation, and screening of strains. Few studies have explored it as a variant of traditional SSF or developed it as a model for studying the physiology of filamentous fungi under SSF conditions[21]. However, the potential of AgSF as a fermentation strategy was rarely evaluated. Additionally, the development of AgSF as a model for physiological studies in SSF, as well as its application as a fermentation method in *M. alpina*, has not been investigated to date.

To gain a comprehensive understanding of the production potential, lipid synthesis capacity, mycelium characteristics and physiological status of AgSF in *M. alpina*, a systematic evaluation of AgSF was conducted using *M. alpina* M0223. First, differences in mycelial characteristics and lipid profiles between AgSF-M0223 and SmF-M0223 were analyzed. Next, the physiological status of mycelium was assessed through comparative transcriptome analysis. Finally, based on these findings, the fermentation process of AgSF-M0223 was optimized. This study aims to provide a new theoretical foundation for the fermentation of *M. alpina*, introduce a novel fermentation strategy for producing ARA-rich lipids, and offer new insights into lipid synthesis by oleaginous microorganisms.

Results

Mycelial characteristic and lipid profile of AgSF- and SmF-cultured *M. alpina* M0223

As shown in Fig. 1a, although the biomass of AgSF-M0223 was slightly lower than that of SmF-M0223, its lipid content was significantly higher, with a 74.26% increase over SmF-M0223 (Fig. 1a). Moreover, ARA comprised 72.53% of total fatty acids (TFAs) in AgSF-M0223, representing a 72.21% increase compared to SmF-M0223, and the ARA content per unit of mycelium was 183.66% higher than in SmF-M0223 (Fig. 1b, c). Additionally, levels of ARA synthesis precursors, including palmitic acid (PA), stearic acid (SA), oleic acid (OA), and linoleic acid (LA), were lower in AgSF-M0223, implying an enhanced conversion efficiency to ARA in AgSF-M0223 (Fig. 1b, c). Overall, the yields of ARA and lipid containing 72.53% ARA in AgSF-M0223 were 4.38 g/L and 7.28 g/L, respectively, representing increases of 141.63% and 48.25% over SmF-M0223 (Fig. 1a).

Morphologically, AgSF-M0223 formed a typical SSF-mycelium network of AH, SH, and penetrative hyphae (PH) embedded in the medium (Fig. 1g). No significant morphological differences were observed between the collected AH and SH. However, the SH was dense, pancake-shaped, and exhibited a higher density than the cotton-like AH, resulting in reduced light transmission. Consistent with this, the biomass of SH was substantially higher than that of AH, while both displayed high ARA content (Fig. 1d-f). Additionally, the morphology of the VH in SmF-M0223 also resembled that of SH, and exhibited a lower density (Fig. 1g). These findings suggested that the high-density SH played a critical role in promoting ARA-rich lipid production by AgSF-M0223.

The lipid and ARA synthesis capacities of AH, SH, and VH were further compared by the changes in lipids, ARA and the precursor fatty acids of ARA over time (Fig. 2a). SH is harvestable after 96 h of cultivation, and it displayed higher levels of lipids, ARA, and major fatty acid precursors compared to VH (Fig. 2b-i). Lipid accumulation in SH was fast from 96 to 120 h (Fig. 2b), accompanied by a rapid increase in ARA (Fig. 2c) and precursor fatty acids (Fig. 2d-i). Following this phase, lipid and ARA accumulation rates slowed, while precursor fatty acid content slowly reduced. VH exhibited a similar accumulation trend, with a prolonged rapid accumulation phase but lower lipid and ARA synthesis rates. AH, which could be harvested after 144 h of cultivation, showed comparable initial lipid and ARA content and consistent temporal change patterns to basal SH, albeit at a slower rate. These results indicated that SH and AH contained higher initial lipid and ARA levels, with SH exhibiting a greater capacity for lipid and ARA accumulation compared to VH. These characteristics contributed to the high ARA-rich lipids of AgSF-M0223.

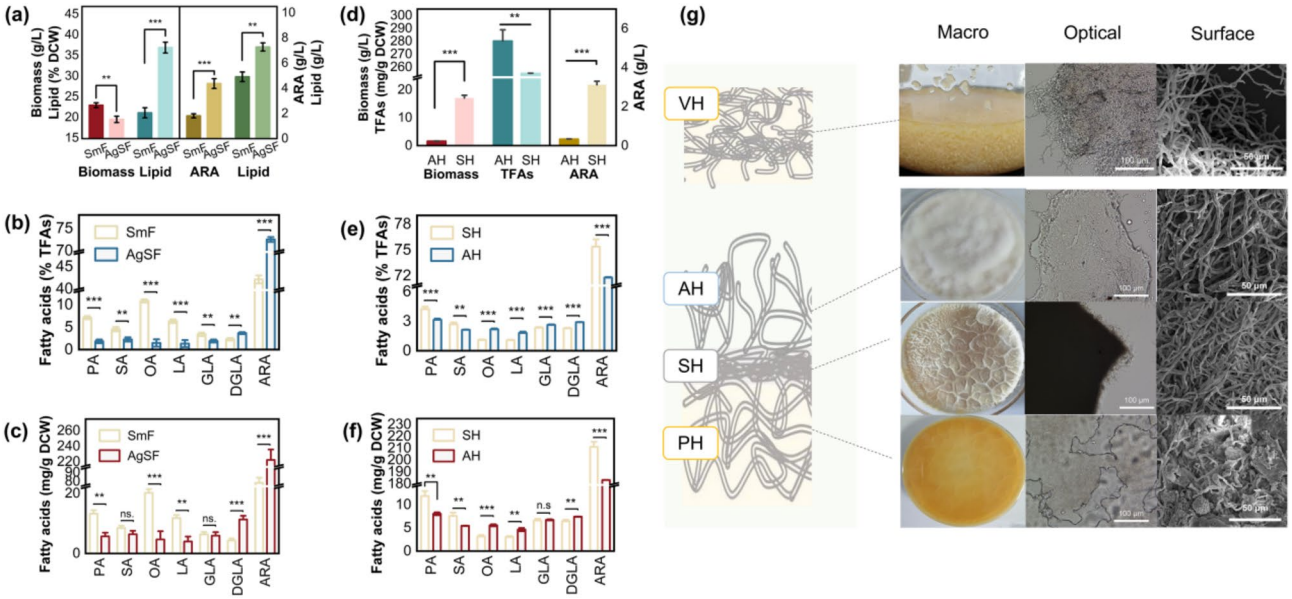

Fig. 1. The comparison of SmF-M0223 and AgSF-M0223. (**a**) Distincts of biomass, lipid and ARA yield, as well as fatty acid composition (**b**) and content (**c**) in dried cell weight (DCW) between SmF-M0223 and AgSF-M0223 ($n = 3$). (d) Biomass, total fatty acid content in DCW and ARA yield differences, as well as fatty acid composition (**e**) and content (**f**) in dried cell weight (DCW) of AH and SH in AgSF-M0223 ($n = 3$). Asterisk at the top of the error bars indicated significant differences between the two groups: * represents $p \leq 0.05$, ** $p \leq 0.01$, *** $p \leq 0.001$, and "ns" denotes no significant difference. (**g**) Macro-morphological (Macro), optical morphological (Optical) and SEM-based surface morphological (Surface) distinctions between VH produced by SmF-M0223, and AH, SH and PH produced by AgSF-M0223. PA, palmitic acid. SA, stearic acid. OA, oleic acid. LA, linoleic acid. GLA, γ-linolenic acid. DGLA, dihomo-γ-linolenic acid. ARA, arachidonic acid.

Transcriptome analysis among AH, SH, and VH in the period of rapid lipid synthesis

RNA-sequencing of AH, SH, and VH

To clarify why AgSF-M0223 produced high levels of ARA-rich lipid, RNA sequencing and analysis of AH, SH, and VH during the rapid lipid synthesis phase was conducted. A total of 68.59 Gb of clean bases was obtained. Over 97.7% of the reads aligned to the *M. alpina* M0223 genome (Table S1). With PCA and Pearson correlation analysis, samples of AH, SH, and VH can be clearly distinguished and have good reproducibility. Moreover, several unique genes expressed in AgSF, especially in AH, suggested a distinct transcriptional profile in AgSF (Fig. S1).

Gene set enrichment analysis between AH, SH, and VH

To further investigate transcriptional differences among AH, SH, and VH, gene set enrichment analysis (GSEA) was performed on all genes (Table S2) between AH vs. VH, SH vs. VH, and SH vs. AH, using genes with Gene Ontology (GO) and Kyoto Encyclopedia of Genes and Genomes (KEGG) annotations as a priori gene sets, respectively (Fig. 3). According to the GSEA results between AH vs. VH (Fig. 3a), the significant down-regulation of energy, carbohydrate, amino acid and cofactor metabolism in KEGG, as well as the biosynthesis and metabolism of nucleotides, cofactors, carbohydrate derivatives and proteins in GO, revealed attenuated primary metabolism in AH. Additionally, multiple GO terms related to ribosomal function (e.g., "ribosome" and "ribonucleoprotein complex") and KEGG pathways for "ribosome" and "aminoacyl-tRNA biosynthesis" were also significantly downregulated in AH, further indicating a weaker protein synthesis in AH. Besides, AH probably underwent less DNA damage based on the downregulation of multiple pathways related to "replication and repair", such as "base excision repair", "DNA replication", and "nucleotide excision repair", etc. Coupled with the downregulation of "glutathione metabolism", a key antioxidant[22], AH might experience lower oxidative stress than VH, potentially mitigating the oxidation of unsaturated fatty acids.

In SH, significantly downregulated pathways related to "replication and repair" and "glutathione metabolism" showed a similar lower oxidative stress to AH (Fig. 3b). However, GSEA using both GO and KEGG gene sets showed upregulation of ribosomal functions in SH. Specifically, terms such as "ribosome" and "non-membrane-bound organelle" in GO, along with "ribosome biogenesis", "ribosome", and "RNA polymerase" in KEGG, were enriched, suggesting enhanced protein synthesis in SH. These physiological statuses were consistent with that of the SSF in the increased enzyme productivity[23]. Additionally, glycerophospholipid and glycerolipid metabolism, which are typically involved in lipid assembly and fatty acids desaturation, were upregulated in SH, prompting an increased capacity for lipid and ARA accumulation in SH. Compared to SH (Fig. 3c), AH exhibited reduced transcriptional and translational activity, including downregulation of ribosomal functions,

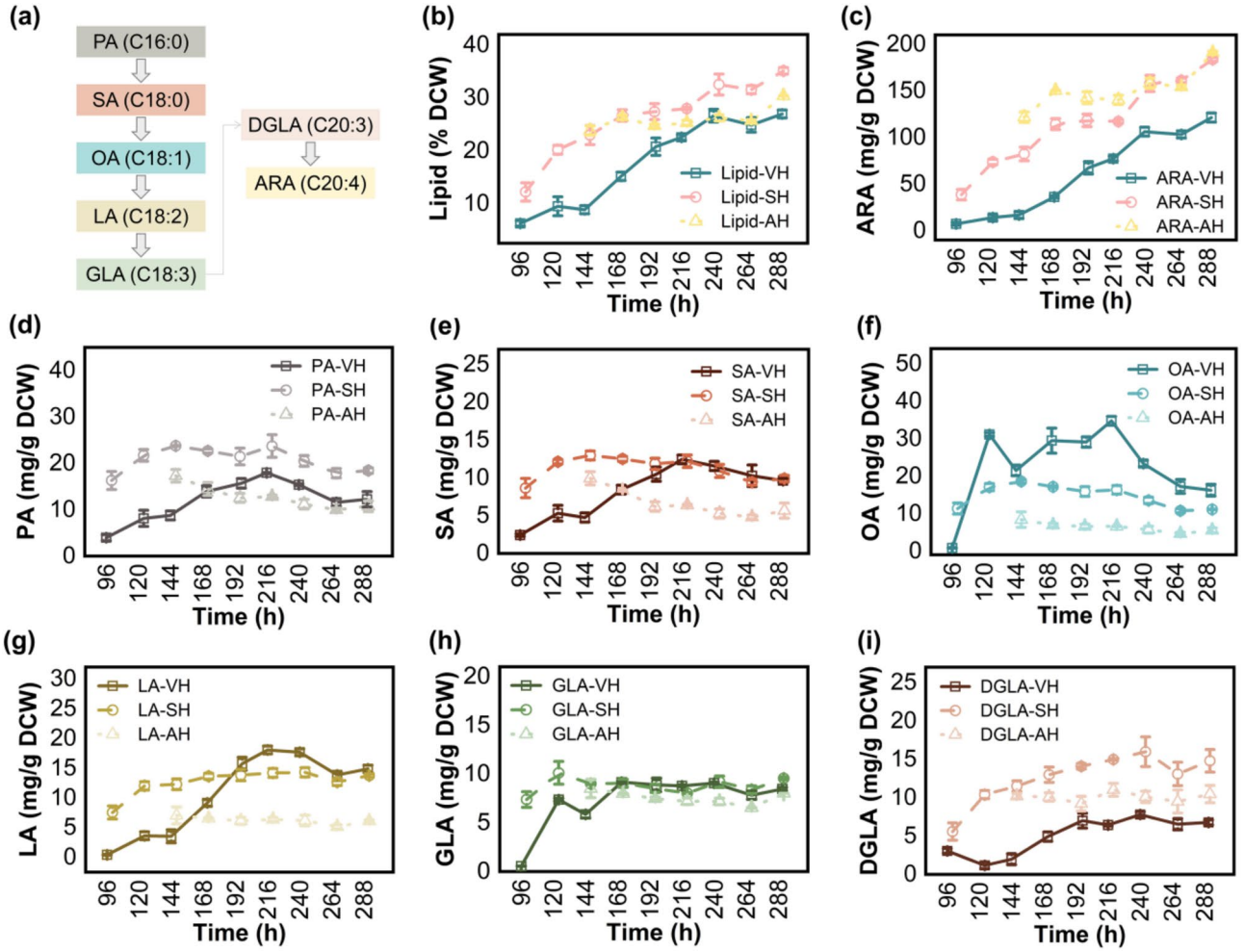

Fig. 2. Time courses of changes in fatty acids content of AH, SH and VH. As shown in (**a**), the synthesis of ARA undergoes a series of elongation and desaturation process from palmitic acid (C16:0, PA), leading to the sequential production of stearic acid (C18:0, SA), oleic acid (C18:1, OA), linoleic acid (C18:2, LA), γ-linolenic acid (C18:3, GLA), dihomo-γ-linolenic acid (C20:3, DGLA) and arachidonic acid (C20:4, ARA). (**b**) The changes of lipid content and major fatty acids content (**c**-**i**) in dried cell weight ($n = 3$).

RNA polymerase activity, regulation, etc. Metabolic pathways such as "glycolysis", "pyruvate metabolism", and "oxidative phosphorylation" were also downregulated, suggesting lower mycelial viability than SH. This further reflected a response in AH to nutrient limitations.

Transcriptional analysis of the lipid metabolism among AH, SH, and VH

Differentially expressed genes (DEGs) associated with lipid metabolism were analyzed. Genes with $p < 0.05$ among AH, SH, and VH were considered DEGs (Table S3). Glycolysis, the starting point for lipid synthesis, was significantly weaker in the AH than in SH and VH, further illustrating AH-restricted nutrition and its limitations on lipid synthesis. Further, according to the GSEA of "glycolysis", SH and VH showed similar glycolytic capacity (Fig. 4a$_1$, a$_2$). However, the citrate cycle was weaker in SH than in VH, leading to more glucose being fluxed towards fatty acid synthesis in SH and more being fully oxidized to CO_2 in VH (Fig. 4b). Furthermore, the genes encoding glucose-6-phosphate dehydrogenase and malic enzyme, critical for NADPH supply, were significantly upregulated[24,25]. This suggested an enhanced NADPH supply in SH (Fig. S2, S3). These physiological features aided in the synthesis of fatty acids. Besides, the transcript levels of desaturase and elongase in SH were lower than in VH but remained abundant (Fig. S4). A similar phenomenon was observed in the study of Yu et al.[26]. These suggested that the abundance of desaturase in *M. alpina* was enough to support the desaturation process. Enhanced triacylglycerol synthesis (Fig. 4d$_1$, d$_2$) and glycerophospholipid metabolism (Fig. 4e$_1$, e$_2$) in SH likely play a more vital role in accelerating fatty acid conversion to ARA-rich lipids. Additionally, the attenuated fatty acid degradation in SH reduced lipid consumption (Fig. 4c). These differences in physiological features collectively contributed to SH's high lipid and ARA accumulation capacity.

Based on the transcriptomic analysis of lipid metabolism pathways (Fig. 4f), the citrate cycle in SH was weakened, while the synthesis of triglycerides and glycerophospholipid metabolism were enhanced. These changes, coupled with glycolytic capacity comparable to that of VH, directed more glucose toward lipid

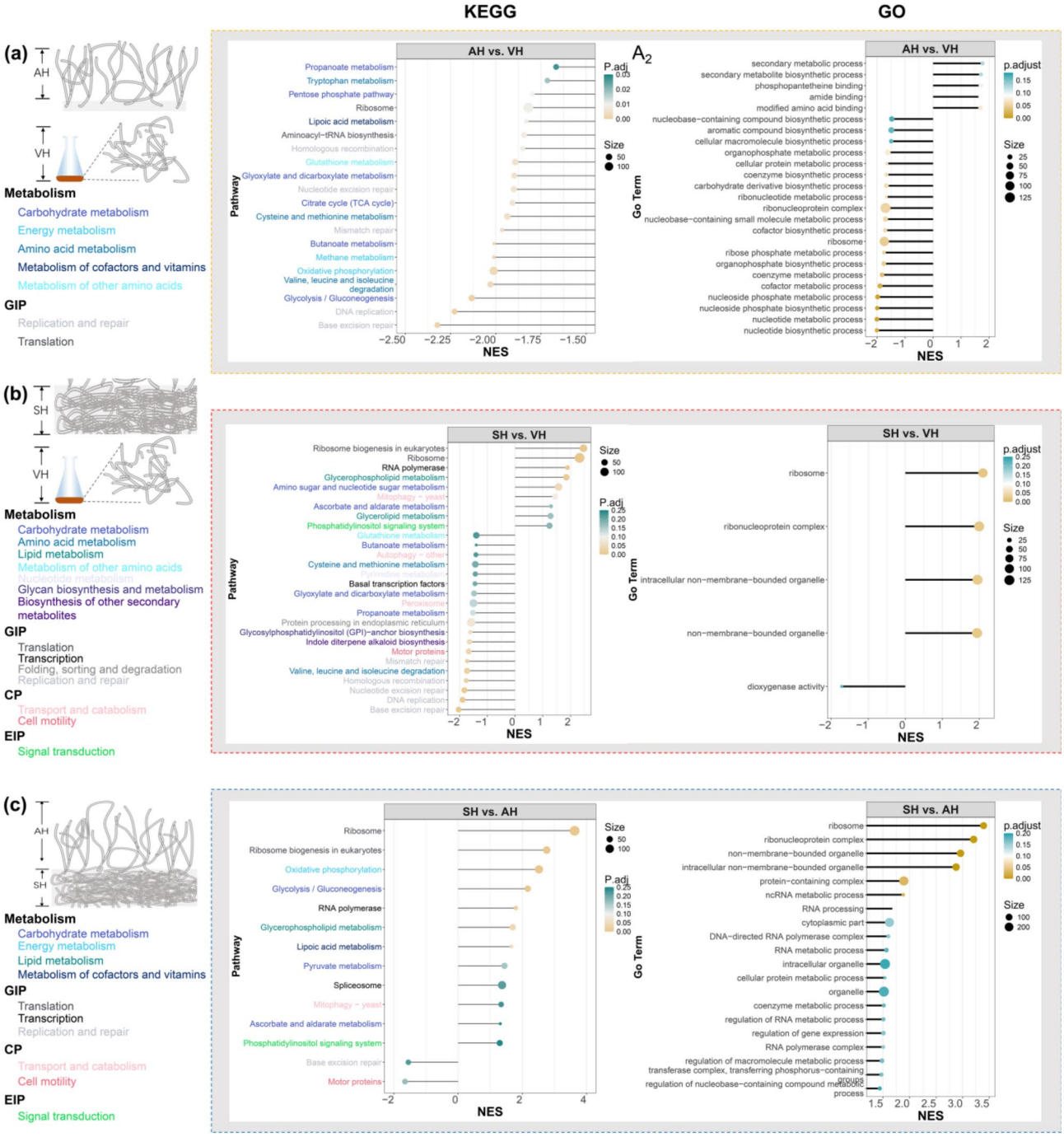

Fig. 3. Gene set enrichment analysis of AH, SH and VH. Significant pathways and GO terms from the GSEA of genes between AH vs. VH (**a**), SH vs. VH (**b**) and SH vs. AH (**c**). $p < 0.05$ and padj < 0.25 were considered significantly enriched. The color gradient from tawny to green represents high to low significance, and the bubble size represents the number of genes contributing to that pathway or GO term.

synthesis. Additionally, fatty acid β-oxidation (FAO) was reduced in SH. Together, these factors contributed to the enhanced lipid synthesis capacity observed in SH. In the study of Krishnan, J. et al.[27], hypoxia was shown to inhibit the citrate cycle and enhance triglyceride synthesis, similar to the effects observed in SH, implying a possible hypoxic microenvironment in SH. To investigate this, we measured the oxygen content in SH and VH during the rapid lipid synthesis phase. The oxygen content in the microenvironment of the SH produced by AgSF-M0223 was 0.048 ± 0.045 mg/L, significantly lower than that in the liquid environment of SmF-M0223, which was 4 ± 0.47 mg/L (Fig. S5). This suggests that the SH of AgSF-M0223 is in a hypoxic microenvironment during the rapid lipid synthesis phase. Furthermore, a liquid superficial-static culture (LSSC) method, a static liquid culture without shaking[28], was employed for *M. alpina* M0223. A fungal mat gradually formed

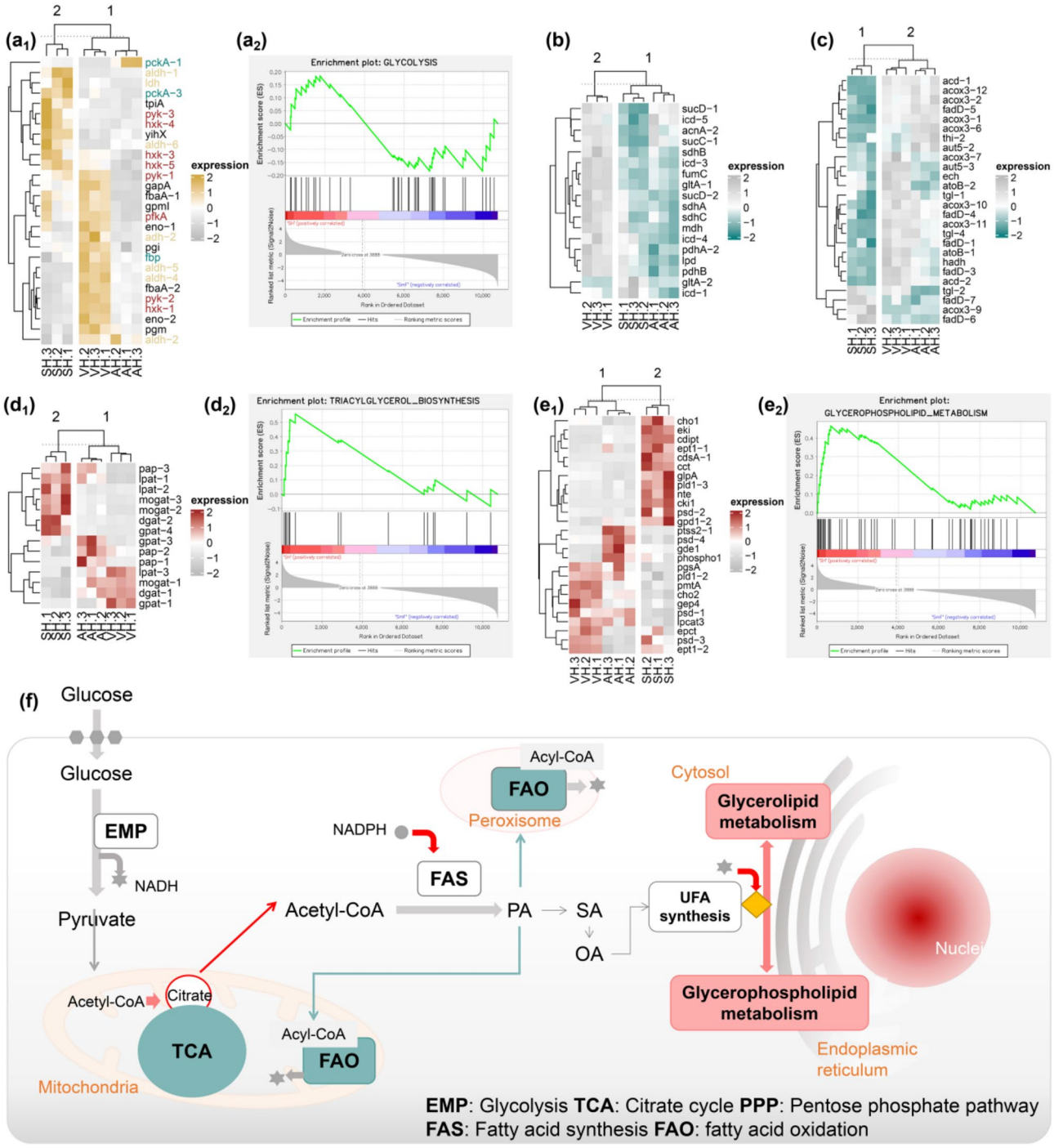

Fig. 4. An overview of transcriptional differences in lipid metabolism pathway among SH, AH and VH. In *M. alpina* M0223 cultured with glucose as carbon source, pyruvate produced from glucose via the EMP pathway undergoes the TCA cycle in the mitochondria to synthesize citrate. When the produced citrate overflows from the TCA cycle, the carbon flux shifts into fatty acid synthesis by fatty acid synthetase (FAS) in the cytoplasm. The synthesized fatty acids subsequently form triglycerides via the Kennedy pathway or enter glycerophospholipid metabolism and are desaturated or elongated in the form of phosphatidylcholine or acyl CoA via the fatty acid desaturase/elongase system. Besides, the synthesized fatty acids can be degraded by mitochondrial and peroxisomal fatty acid β-oxidation (**f**). Heatmap of genes with significant differences among AH, SH and VH in EMP ($\mathbf{a}_1$), TCA (**b**), FAO (**c**), triacylglycerol biosynthesis ($\mathbf{d}_1$) and glycerophospholipid metabolism ($\mathbf{e}_1$). GSEA results of glycolysis ($\mathbf{a}_2$), triacylglycerol biosynthesis ($\mathbf{d}_2$) and glycerophospholipid metabolism ($\mathbf{e}_2$) between SH and VH.

at LSSC-M0223 (Fig. S6), which exhibited biomass comparable to that of AgSF-M0223. Although the lipid and ARA yields were lower than those from AgSF-M0223, they were still significantly higher than those from SmF-M0223, increasing by 48.63% and 108.42%, respectively (Fig. S6). These results further underscore the critical role of SH in lipid accumulation under specific physiological conditions.

Enhancing lipid accumulation and growth in AH via improved nutrient availability

According to transcriptomic and lipid profile analyses, lipid synthesis in the AH could be limited by the scarcity of glucose, the starting point for lipid synthesis. A medium spraying strategy was used to provide direct nutrients to the AH. Following this spraying, the expression of genes encoding key enzymes in glucose transport (*glut*-1), glycolysis (*hxk*-2, *hxk*-5, and *pfk*), and the citrate cycle (*acnA*, *icd*, and *sucA*) was upregulated, (Fig. 5a, b). After 72 h of spraying, the increases in total fatty acids and ARA in AH exceeded those observed in the control group. These indicated enhanced glucose utilization promoted the ability to synthesize fatty acids and ARA in AH (Fig. 5e, f). Similarly, the expression of *glut*-3, *glut*-4 and glycolytic enzymes in SH was also upregulated, albeit to a lesser extent than in AH (Fig. 5c). But unlike in AH, the expression of key enzymes in the citrate cycle remained unchanged (Fig. 5d). After spraying, SH also showed significant increases in total fatty acids and ARA levels (Fig. 5e, f), suggesting that the optimization of nutrients would further promote fatty acid and ARA synthesis in SH.

Effect of various nutrient component concentrations on AgSF-M0223

Nutrient levels significantly influence carbon flow toward lipid accumulation or growth within the mycelium. As shown in Fig. 6a$_1$, biomass and lipid accumulation in AgSF-M0223 advanced gradually with increasing glucose concentration, but excessive glucose concentration inhibits mycelial growth (Fig. 6a$_2$). A broader glucose concentration of 40–80 g/L is capable of producing lipids with high ARA content, and 80 g/L is the highest concentration for growth and lipid accumulation.

Nitrogen is essential in the synthesis of cellular components such as amino acids and nucleotides, whereas nitrogen deprivation promotes lipid accumulation[29]. In AgSF-M0223, nitrogen concentration demonstrated a positive correlation with growth (Fig. 6b$_1$), and excess nitrogen resulted in thicker SH and less AH (Fig. 6b$_2$). Lipid content decreased rapidly at yeast extract concentrations above 9 g/L. Whereas, below 9 g/L, the content and yield of ARA demonstrated a positive correlation with nitrogen availability (Fig. 6b$_1$). 9 g/L is suitable for producing ARA-rich lipid. Besides, similar to the high OA content of 100 g/ L and the high PA content of 20 g/ L, excessively high or low nitrogen concentrations resulted in distinct fatty acid compositions, implying that extreme nutrient concentrations could lead to unusual mycelial status (Fig. 6b$_1$).

The effect of inorganic salt was evaluated by adjusting its concentration while keeping the ratio constant. Inorganic salt concentration mainly affected biomass rather than lipid content and fatty acid composition (Fig. 6c$_1$). Mycelial growth was inhibited at concentrations higher than 5× (Fig. 6c$_2$). Both too-high (> 4×) and low (< 3×) concentrations resulted in reduced biomass and lower yields of ARA and lipids (Fig. 6c$_1$). Therefore, a proper concentration (3 ×) was determined.

After integrating the optimal concentrations of each nutrient component, the yields of ARA and lipid reached 5.61 g/L and 11.12 g/L, respectively, without changing the fatty acid composition, which was 25.22% and 43.48% higher than the control. Further, the yield of lipids and ARA increased to 12.64 g/L and 7.28 g/L after the coupled

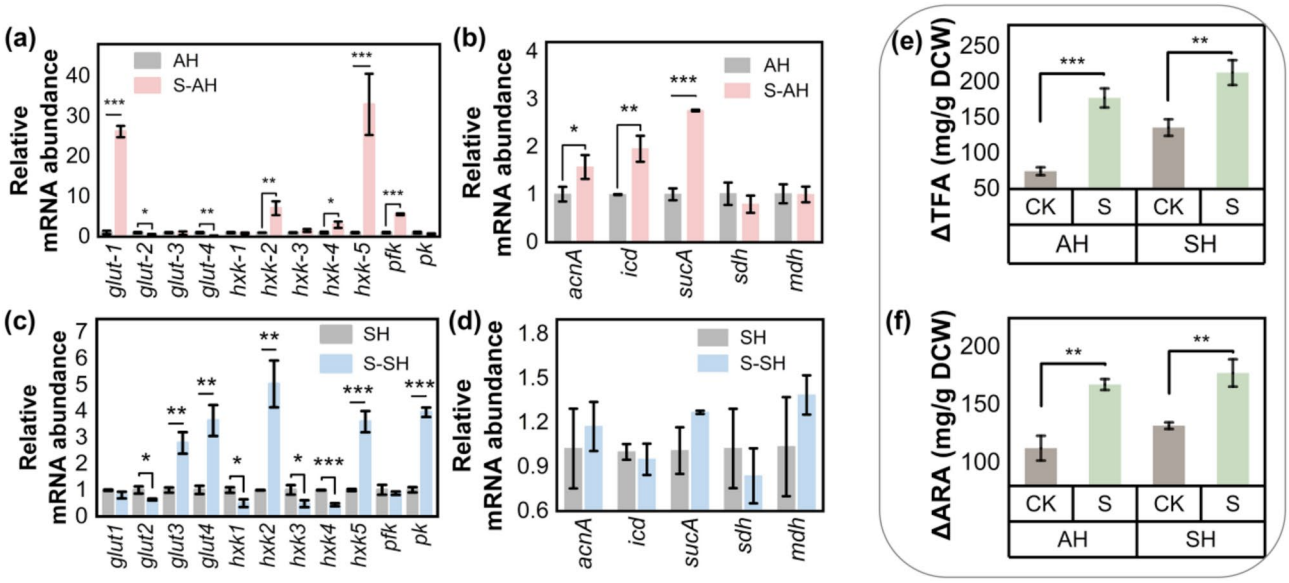

Fig. 5. The effect of spraying medium on AH and SH. The expression level of genes encoding key enzymes in EMP (**a**) and TCA (**b**) of AH and SH (**c, d**) after spraying for 3 h ($n = 6$). (**e**) Differences in increments of TFA and ARA (**f**) in AH and SH after 72 h of spraying medium ($n = 3$).

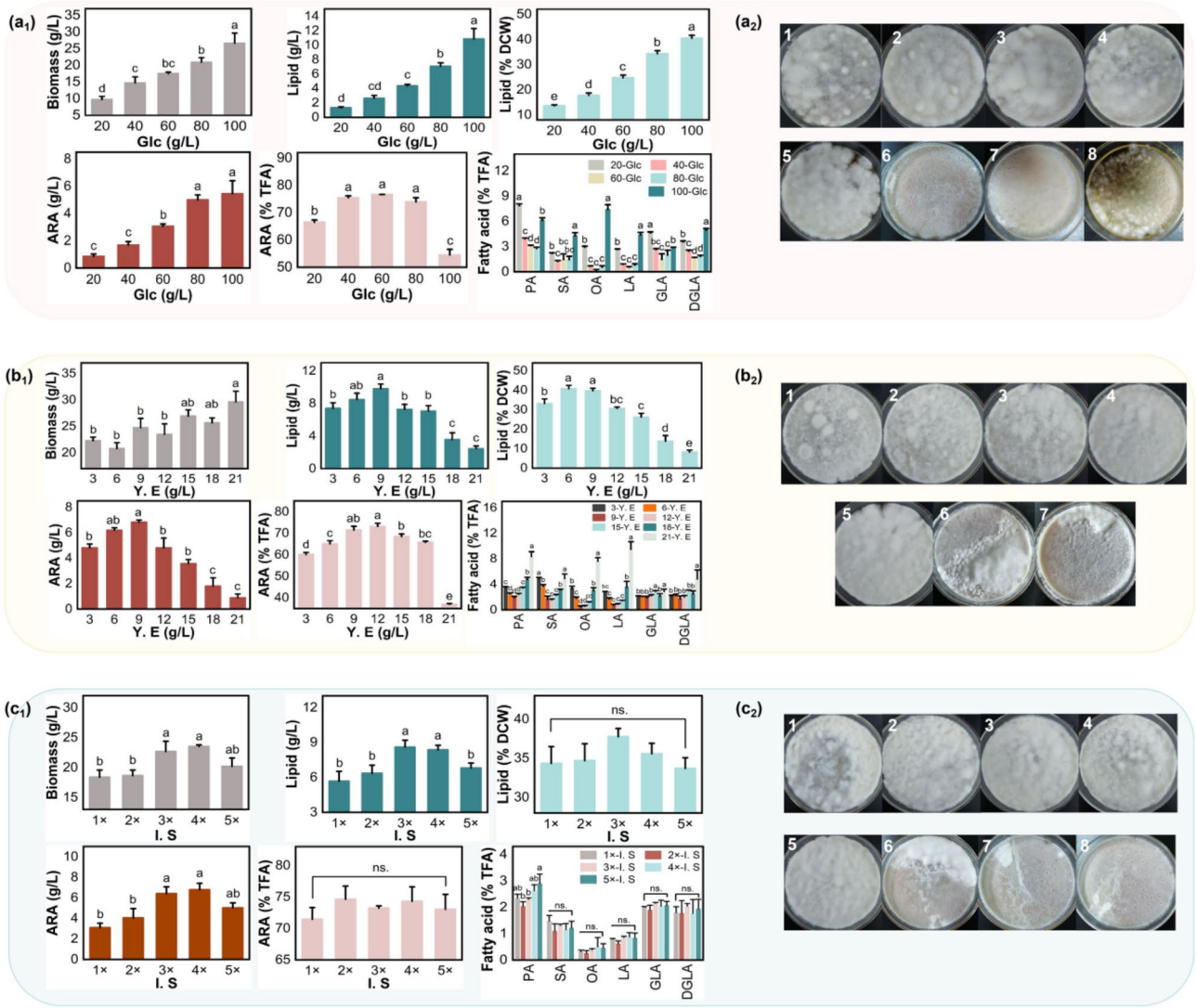

Fig. 6. The effect of nutrients concentration on AgSF-M0223. ($\mathbf{a}_1$) The distinct of biomass, lipid, ARA and fatty acid composition of AgSF-M0223 under different glucose concentration of 20, 40, 60, 80, 100, 120, 160, 200 g/L, ($\mathbf{b}_1$) yeast extract concentration of 3, 6, 9, 12, 15, 18, 21 g/L and ($\mathbf{c}_1$) inorganic concentration of 1×, 2×, 3×, 4×, 5×, 8×, 10×, 12 × (0.6 g/L of $NaNO_3$: 0.6 g/L KH_2PO_4: 0.1 g/L $MgSO_4{\cdot}7H_2O$) ($n = 3$), as well as their macroscopic morphology ($\mathbf{a}_2$, $\mathbf{b}_2$, $\mathbf{c}_2$). Numbers from low to high represent the macroscopic morphology of AgSF-M0223 from low to high concentrations. Groups that do not share the same letter are significantly different from each other ($p \leq 0.05$), while 'ns' indicates no significant difference overall, according to the Bonferroni method.

medium spraying strategy (48 h interval spraying implemented after 8 days of incubation), which was 13.67% and 29.77% higher than that of the unsprayed group, and the fatty acid composition was not affected (Table S4). These indicated that AgSF enhanced both ARA and lipid yields, making it suitable for ARA-rich lipid production.

Discussion

SSF is an eco-friendly technology for cultivating diverse saprophytic fungi to produce high-yield bioactive compounds, enzymes, and other valuable products[30–32]. In this study, we suggested that AgSF, a special SSF, was a promising eco-friendly strategy for ARA-rich lipid production in *M. alpina*. Further, new insights into the association between ARA-rich lipid accumulation and the physiological status of *M. alpina* in AgSF were clarified. This deepened the understanding of fungal physiology in SSF and advanced applications for ARA-rich lipid production.

Fungi are well adapted to grow on surfaces[33]. SSF-cultured filamentous fungi form a three-dimensional mycelial network containing SH and, in some filamentous fungi (e.g., Aspergillus), biofilms[21,34]. Unlike SmF, where nutrients and oxygen are uniformly distributed, there are inevitable substrate, enzyme, and oxygen concentration gradients in the substrate and fungal mat of SSF, contributing to the special microenvironmental and physiological status of the biofilm[35,36] In *Aspergillus fumigatus*, oxygen content within the biofilm decreased

rapidly with increasing density, and there was a steep decline in oxygen levels with increasing depth from the air interface, resulting in a hypoxic microenvironment[37,38]. Consistent with this, SH produced by AgSF during the rapid lipid synthesis phase is also in a hypoxic microenvironment. Hypoxia has important regulatory roles in lipid metabolism. Up-regulated hypoxia-inducible factor (HIF) 1α inhibits the citrate cycle and activates glycolytic genes and PPARγ, whose products, in turn, activate glycerolipid biosynthesis genes, thereby facilitating carbon flux toward lipid synthesis[27,39]. The attenuated citrate cycle and enhanced triacylglycerol synthesis in SH hinted at a possible role of the hypoxic microenvironment in *M. alpina* in efficiently directing carbon flux toward lipid synthesis.

Based on the fatty acid desaturase/elongase system, arachidonic acid (ARA) synthesis involves a series of elongation and desaturation processes. These processes are catalyzed by elongase, Δ9 fatty acid desaturase, Δ12 fatty acid desaturase, Δ6 fatty acid desaturase, Δ6 elongase, and Δ5 fatty acid desaturase, starting from palmitic acid (C16:0, PA) and leading to the sequential production of stearic acid (C18:0, SA), oleic acid (C18:1, OA), linoleic acid (C18:2, LA), γ-linolenic acid (C18:3, GLA), dihomo-γ-linolenic acid (C20:3, DGLA), and finally, ARA (C20:4). Fatty acid desaturases are key enzymes in the ARA synthesis pathway, but the transcription levels were down-regulated in SH compared to VH. Microorganisms can finely regulate unsaturated fatty acid (UFA) synthesis in response to environmental factors. Previous studies have shown that fatty acids and oxygen regulate the transcript levels and mRNA stability of the gene encoding Δ9 fatty acid desaturase (ole1) via the fatty acid response element and hypoxia response element in the ole1 promoter. However, the transcriptional activation of both elements is suppressed by unsaturated fatty acids[40]. Moreover, environmental factors such as temperature and osmotic pressure can influence desaturase gene expression. For instance, low temperatures up-regulate mRNA levels of desaturase in *Saccharomyces cerevisiae*[41], while high salt concentrations decrease gene expression in *Hortaea werneckii*[42]. The regulatory mechanisms behind the decreased transcript levels of fatty acid desaturases in SH produced by AgSF-M0223 remain unclear. However, it is possible that the inherently high transcript and protein abundance of fatty acid desaturases in *M. alpina* means that their down-regulation has a minimal effect on ARA synthesis, as observed in this study and in a previous study by Yu et al.[26]. In addition to fatty acid desaturases, glycerophospholipid metabolism plays a crucial role in fatty acid desaturation. In eukaryotes with a fatty acid desaturase/elongase enzyme system, such as *Mucor circinelloides* and certain plants, oleoyl-CoA must bind to phosphatidylcholine before being used as a substrate for desaturase to synthesize C18:2 or C18:3[43]. Hypoxia has been shown to enhance phospholipid metabolism, thereby increasing the content of unsaturated fatty acids in plants[45,46]. Moreover, C18 polyunsaturated fatty acid (PUFA) levels were increased after enhancing the channeling of PC-modified fatty acids into the DAG pool by heterologous expression of PDCT[47]. Enhanced glycerophospholipid metabolism under SH should also play a key role in ARA synthesis. These suggested a potential role for hypoxic environments of oleaginous microorganisms in the production of ARA-rich lipid synthesis.

Furthermore, consistent with the high protein synthesis capacity demonstrated by eukaryotic SSF, ribosomal function was significantly enhanced, and amino acid degradation (particularly, leucine) was weaker in SH. Ribosomes are complexes that synthesize proteins from amino acids and are tightly regulated by nutritional availability in the environment (e.g. leucine, arginine and glutamine) by the target of rapamycin (TOR) signalling[48]. During nutritional stress, translation of ribosomal proteins is strongly inhibited and degraded[49]. Evidently, ribosomal functions such as r-protein synthesis and nucleolus were significantly down-regulated in nutritionally restricted AH. It is implied that nutritional availability in the environment could be the reason why eukaryotic SSFs exhibit high protein synthesis capacity.

The special physiological status of AgSF-M0223 conferred a higher yield of ARA-rich lipid than SmF-M0223. Meanwhile, AgSF, a special SSF, did not involve the stirring required for SmF, as well as the discharge and treatment of wastewater[6]. Moreover, it could avoid the heat and mass transfer issues and substrate heterogeneity associated with traditional SSF, which often leads to unstable product quality and contamination[20]. Further, LSSC results showed that the formation of biofilm was crucial to the high lipid-accumulation capacity of AgSF. Therefore, some gelling agents have the potential to be used as alternatives to agar to further reduce costs, such as carboxymethyl cellulose, xanthan gum, and polyvinylpyrrolidone[50–52]. Also, even without the use of gelling agents, direct superficial-static culture was feasible. What's more, an automated scale-up system for AgSF has been developed, integrating sterilization and cultivation processes[53]. Based on the superior performance of SH accumulating ARA-rich lipid, some biofilm reactors possibly could be available as well[54]. Advances in mechanical automation would lead to the further development of new gel fermentation equipment. Therefore, the advantages of AgSF-M0223's high yield of ARA-rich lipid and eco-friendly could be magnified in the booming landscape of artificial intelligence and automation.

Conclusions

In this study, AgSF was developed for the high yield of ARA-rich lipid in *M. alpina*. Enhanced lipid synthesis in SH and higher starting lipid and ARA content in AH and SH compared to VH together contributed to the superiority of AgSF-M0223. The similar glycolysis, attenuated citrate cycle, and enhanced triacylglycerol synthesis and glycerophospholipid metabolism of SH over VH enhanced glucose flux towards lipid synthesis. Concurrently, down-regulation of fatty acid degradation reduced lipid depletion in SH. AH, on the other hand, exhibited weaker primary metabolism due to restricted nutrients, limiting lipid accumulation. Building on these insights, optimization of AgSF with a spraying strategy further enhanced the ARA-rich lipid production capacity of AgSF-M0223, achieving 12.64 g/L of lipids with 70.41% ARA. This study provided new insights into ARA-rich lipid production mechanisms on SSF and a promising eco-friendly fermentation strategy.

Methods

Microorganism and medium

M. alpina M0223, preserved in our laboratory, was kept on potato dextrose agar (PDA) to ensure strain conservation and obtain spores for fermentation. The fermentation medium contained 80 g/L glucose, 12 g/L yeast extract, 3 g/L $NaNO_3$, 3 g/L KH_2PO_3, and 0.5 g/L $MgSO_4{\cdot}7\ H_2O$, with 15 g/L agar for AgSF and no agar for SmF and LSSC. To analyze the effects of nutrient concentration, glucose, yeast extract, and inorganic salt levels were varied individually while keeping the concentrations of other components constant. The spraying medium composition was identical to that of AgSF.

Culture method

The culture method was performed as previously described[55]. Briefly, *M. alpina* M0223 was cultured on PDA plates for 8 days, and the spore suspension was then inoculated into the fermentation medium at 10% of the medium volume. The cultures were incubated in (80 ml/250 ml) triangular flasks at 28 °C, 180 rpm for 12 days for SmF. For AgSF, 20 mL of sterilized fermentation medium containing agar was spread evenly on a 90 mm diameter plate to a height of approximately 0.36 cm. The plate was then inoculated with a 10% (v/v) spore suspension and incubated at 28 °C for 12 days. Medium spraying was performed on the third day after the fungal mat had formed (on the eighth day of incubation) using a sterile spray bottle, which contained 1.5 mL of the spray medium. Each plate received 1.5 mL of the medium per spray. The spraying intervals varied in the optimization experiments and included 12, 24, 36, 48, 60, and 72 h between each spray. For LSSC, the spore suspension (10% inoculum) was added to fermentation medium without agar, and 20 mL of the mixture was spread evenly onto a 90 mm plate, followed by incubation at 28 °C for 12 days.

Determination of dry cell weight, total lipid, and fatty acid profiles

To determine the dry cell weight, the vegetative hyphae (VH) in SmF were harvested by filtration, while the mycelium in AgSF was collected by scraping from the surface of agar plates, comprising the aerial hyphae (AH) and surface hyphae (SH). Due to that SH forms a tightly wound mycelial mat while AH consists of a fluffy mycelium growing on top of SH, they can be easily separated. The SH, after the removal of AH, is shown in Fig. S7. The collected mycelium was dried at 60 °C to constant weight. The determination of total lipid was performed as described in reported studies using n-hexane as an extractive agent[56]. Fatty acid profiles were detected with a simple modification of the method of Chen et al.[57] and Yin et al.[58]. In brief, methylation of fatty acids was performed by boron trifluoride (BF3) using pentadecanoic acid as a standard. Further, the obtained fatty acid methyl esters (FAMEs) were analyzed by a Gas Chromatography system (CLARUS 680, PerkinElmer) equipped with Flame Ionization Detector (FID), taking nitrogen as carrier gas. A capillary column (HP-FFAP, 30 m× 0.32 mm ID × 0.25 μm film) was used and the column temperature was increased from the initial 150 °C to 220 °C at a rate of 10 °C/min and maintained at 220 °C for 10 min. The temperatures of the inlet and detector ports were both set at 250 °C. The injection volume was 1 μL. After collecting the peak area data using appropriate software, the percentage of the target FAME (ARA) in total fatty acids was calculated by dividing the area of the ARA peak by the total area of all peaks, then multiplying this result by 100. The content of ARA in dry cell weight (DCW) was determined by dividing the ARA peak area by the pentadecanoic acid peak area, and then multiplying the result by the amount of pentadecanoic acid added[59]. Furthermore, for a better comparison between AgSF-M0223 and SmF-M0223, the yield of ARA, lipids, and biomass in AgSF-M0223 is expressed as the amount of ARA and lipids, as well as dry cell weight harvested from 1 L of agar-containing fermentation medium. The plate specifications used in this study were 90 mm in diameter (with an agar surface area of approximately 55 cm^2, allowing for the conversion of volume to surface area (1 L of medium provides approximately 0.277 m^2 of agar plate). This enables the calculation of yield in g/m^2 surface area, facilitating comparison with other SSF systems. Additionally, the height of the culture medium (approximately 0.36 cm) was determined based on the 20 mL volume used, and the container size can be adjusted accordingly.

Morphology observation by optical microscopy and scanning electron microscope

The optical morphology of *M. alpina* M0223 was observed using a biological microscope (BX53, Olympus). Before scanning electron microscope analysis (SEM), samples were initially fixed overnight in 2.5% glutaraldehyde, and then underwent gradient dehydration with ethanol concentrations from 30 to 100%, with two washes at 100% ethanol. Subsequently, ethanol was replaced with isoamyl acetate, and samples were lyophilized overnight. The dried samples were sputter-coated with gold for 300 s. SEM images were collected with a Nova NanoSEM 450 (FEI, Holland).

Transcriptome analysis

SH, AH, and VH in the rapid lipid and ARA synthesis period were collected and snap-frozen by liquid nitrogen. Then, RNA was extracted by the RNA Isolation Kit (Beibei Biotechnology) and RNA integrity and quality were assessed by Nanodrop and agarose gel electrophoresis. RNA sequencing was performed by the DNBSEQ-T7 platform. Transcript expression levels were quantitatively analyzed using TPM (transcripts per million reads) as the quantitative index with RSEM[60]. Gene Ontology (GO)[61,62] and the Kyoto Encyclopedia of Genes and Genomes (KEGG)[63,64] databases were utilized for the functional annotation of genes and the enrichment analysis of GO and KEGG were performed by Gene Set Enrichment Analysis (GSEA)[65]. The principal component analysis (PCA), correlation analysis, Venn analysis, and GSEA were performed on the online platform of Major Cloud Platform (https://cloud.majorbio.com/). Displays of GSEA results were done through the R package (ggplot2)[66].

RNA extract and quantitative polymerase chain reaction (RT-qPCR) analysis

Collected mycelium was snap-frozen in liquid nitrogen and then ground into powder with liquid nitrogen. RNA was extracted by RNA Isolation Kit (Beibei Biotechnology). After integrity and quality detection by agarose gel electrophoresis and Nanodrop, cDNA was obtained by HiScript III 1st Strand cDNA Synthesis Kit (+ gDNA wiper, Vazyme). Quantitative Real-time PCR (qRT-PCR) of key enzymes in glycolysis and citrate cycle was performed by StepOne™ System with SYBR Green Fast qPCR Mix (ABclonal). The relative expression levels of the genes were determined by $2^{-\Delta\Delta Ct}$, taking 18 S rRNA as internal control. The primers of qRT-PCR were listed in Table S5.

Detection of oxygen content

After AgSF-M0223 and SmF-M0223 were cultured to the rapid lipid synthesis phase, the oxygen content was measured. The oxygen content in the microenvironment of SH produced by AgSF-M0223 was determined using a microelectrode system connected to an oxygen microsensor (Unisense). In contrast, the oxygen content in the liquid environment of SmF-M0223 was measured using a portable dissolved oxygen meter (HACH).

Statistics analysis

Each experiment used three biological replicates. The analysis between two groups of data was achieved by one-way analysis of variance (ANOVO) in IBM SPSS. The analysis among multiple groups of data was obtained by Bonferroni. $P < 0.05$ was considered to significant difference.

Data availability

All sequencing data are available through the National Center for Biotechnology Information Sequence Read Archive under the accession number PRJNA1191033.

Received: 25 November 2024; Accepted: 2 May 2025
Published online: 07 May 2025

References

1. Harayama, T. & Shimizu, T. Roles of polyunsaturated fatty acids, from mediators to membranes. *J. Lipid Res.* **61**, 1150–1160 (2020).
2. Hanna, V. S. & Hafez, E. A. A. Synopsis of arachidonic acid metabolism: A review. *J. Adv. Res.* **11**, 23–32 (2018).
3. Mamani, L. D. G., Magalhães, A. I., Ruan, Z., de Carvalho, J. C. & Soccol, C. R. Industrial production, patent landscape, and market trends of arachidonic acid-rich oil of *Mortierella alpina*. *Biotechnol. Res. Innov.* **3**, 103–119 (2019).
4. Ghazani, S. M. & Marangoni, A. G. Microbial lipids for foods. *Trends Food Sci. Technol.* **119**, 593–607 (2022).
5. Chang, L. et al. Lipid metabolism research in oleaginous fungus *Mortierella alpina*: current progress and prospects. *Biotechnol. Adv.* **54**, 107794 (2022).
6. Soccol, C. R. et al. Recent developments and innovations in solid state fermentation. *Biotechnol. Res. Innov.* **1**, 52–71 (2017).
7. ul-Haq, I., Idrees, S. & Rajoka, M. I. Production of lipases by *Rhizopus oligosporous* by solid-state fermentation. *Process Biochem.* **37**, 637–641 (2002).
8. Karimi, K., Emtiazi, G. & Taherzadeh, M. J. Ethanol production from dilute-acid pretreated rice straw by simultaneous saccharification and fermentation with *Mucor indicus*, *Rhizopus oryzae*, and *Saccharomyces cerevisiae*. *Enzyme Microb. Technol.* **40**, 138–144 (2006).
9. Verduzco-Oliva, R. & Gutierrez-Uribe, J. A. Beyond enzyme production: solid state fermentation (SSF) as an alternative approach to produce antioxidant polysaccharides. *Sustainability* **12**, 495 (2020).
10. Feng, X., Ng, K., Ajlouni, S., Zhang, P. & Fang, Z. Effect of solid-state fermentation on plant-sourced proteins: A review. *Food Reviews Int.* **40**, 2580–2617 (2024).
11. Vandenberghe, L. P. S. et al. Solid-state fermentation technology and innovation for the production of agricultural and animal feed bioproducts. *Syst. Microbiol. Biomanuf.* **1**, 142–165 (2021).
12. Jovanovic, S., Dietrich, D., Becker, J., Kohlstedt, M. & Wittmann, C. Microbial production of polyunsaturated fatty acids — high-value ingredients for Aquafeed, superfoods, and pharmaceuticals. *Curr. Opin. Biotechnol.* **69**, 199–211 (2021).
13. Qiao, W. et al. Microbial oil production from solid-state fermentation by a newly isolated oleaginous fungus, *Mucor circinelloides* Q531 from mulberry branches. *Royal Soc. Open. Sci.* **5**, 180551 (2018).
14. Zhang, J. & Hu, B. Solid-State fermentation of *Mortierella Isabellina* for lipid production from soybean hull. *Appl. Biochem. Biotechnol.* **166**, 1034–1046 (2012).
15. Certik, M. & Adamechova, Z. Cereal-based bioproducts containing polyunsaturated fatty acids. *Lipid Technol.* **21**, 250–253 (2009).
16. Ferreira, M. et al. Bio-enrichment of oilseed cakes by *Mortierella alpina* under solid-state fermentation. *LWT* **134**, 109981 (2020).
17. Stred'anská, S., Slugeň, D., Stred'anský, M. & Grego, J. Arachidonic acid production by *Mortierella alpina* grown on solid substrates. *World J. Microbiol. Biotechnol.* **9**, 511–513 (1993).
18. Slaný, O. et al. Biotransformation of animal fat-by products into ARA-enriched fermented bioproducts by solid-state fermentation of *Mortierella alpina*. *J. Fungi (Basel).* **6**, 236 (2020).
19. Antimanon, S., Chamkhuy, W., Sutthiwattanakul, S. & Laoteng, K. Efficient production of arachidonic acid of *Mortierella* Sp. by solid-state fermentation using a combinatorial medium with Sp.nt mushroom substrate. *Chem. Pap.* **72**, 2899–2908 (2018).
20. Ooijkaas, L. P., Weber, F. J., Buitelaar, R. M., Tramper, J. & Rinzema, A. Defined media and inert supports: their potential as solid-state fermentation production systems. *Trends Biotechnol.* **18**, 356–360 (2000).
21. Barrios-González, J. & Tarragó-Castellanos, M. R. Solid-state fermentation: Special physiology of fungi. In *Fungal Metabolites* (eds. Mérillon, J.-M. & Ramawat, K. G.). 319–347. https://doi.org/10.1007/978-3-319-25001-4_6 (Springer, 2017).
22. Gasmi, A. et al. An update on glutathione's biosynthesis, metabolism, functions, and medicinal purposes. *Curr. Med. Chem.* **31**, 4579–4601 (2024).
23. Zhao, G. et al. Proteinase and glycoside hydrolase production is enhanced in solid-state fermentation by manipulating the carbon and nitrogen fluxes in *Aspergillus oryzae*. *Food Chem.* **271**, 606–613 (2019).
24. Zhang, H., Cui, Q. & Song, X. Research advances on arachidonic acid production by fermentation and genetic modification of *Mortierella alpina*. *World J. Microbiol. Biotechnol.* **37**, 4 (2021).
25. Hao, G. et al. Role of malic enzyme during fatty acid synthesis in the oleaginous fungus *Mortierella alpina*. *Appl. Environ. Microbiol.* **80**, 2672–2678 (2014).
26. Yu, Y. et al. Mechanism of arachidonic acid accumulation during aging in *Mortierella alpina*: A large-scale label-free comparative proteomics study. *J. Agric. Food Chem.* **64**, 9124–9134 (2016).

27. Krishnan, J. et al. Activation of a HIF1alpha-PPARgamma axis underlies the integration of glycolytic and lipid anabolic pathways in pathologic cardiac hypertrophy. *Cell. Metab.* **9**, 512–524 (2009).
28. Wang, Q. et al. Transcriptome dynamics and metabolite analysis revealed the candidate genes and regulatory mechanism of Ganoderic acid biosynthesis during the liquid superficial-static culture of *Ganoderma lucidum*. *Microb. Biotechnol.* **14**, 600–613 (2021).
29. Fazili, A. B. A. et al. *Mucor circinelloides*: a model organism for oleaginous fungi and its potential applications in bioactive lipid production. *Microb. Cell. Fact.* **21**, 29 (2022).
30. Arapoglou, D. et al. Nutritional upgrade of Olive mill stone waste, walnut shell and their mixtures by applying solid state fermentation initiated by *Pleurotus ostreatus*. *Sci. Rep.* **14**, 13446 (2024).
31. Carvalho, J. K. et al. Production of fermented solid containing lipases from *Penicillium polonicum* and its direct use as biocatalyst in the synthesis of Ethyl oleate. *Bioenerg Res.* **17**, 2440–2449 (2024).
32. Sandoval, J. F., Gallagher, J., Rodriguez-Garcia, J., Whiteside, K. & Bryant, D. N. Improved nutritional value of surplus bread and perennial ryegrass via solid-state fermentation with *Rhizopus oligosporus*. *Npj Sci. Food*. **8**, 95 (2024).
33. Harding, M. W., Marques, L. L. R., Howard, R. J. & Olson, M. E. Can filamentous fungi form biofilms? *Trends Microbiol.* **17**, 475–480 (2009).
34. Carvalho, F. M., Azevedo, A., Ferreira, M. M. Mergulhão, F. J. M. & Gomes, L. C. Advances on bacterial and fungal biofilms for the production of added-value compounds. *Biology* **11**, 1126 (2022).
35. Rahardjo, Y. S. P., Tramper, J. & Rinzema, A. Modeling conversion and transport phenomena in solid-state fermentation: A review and perspectives. *Biotechnol. Adv.* **24**, 161–179 (2006).
36. Viniegra-González, G. & Favela-Torres, E. Why solid-state fermentation seems to be resistant to catabolite repression? *Food Technol. Biotechnol.* **44**, 3 (2005).
37. Oostra, J., le Comte, E. P., van den Heuvel, J. C., Tramper, J. & Rinzema, A. Intra-particle oxygen diffusion limitation in solid-state fermentation. *Biotechnol. Bioeng.* **75**, 13–24 (2001).
38. Kowalski, C. H., Morelli, K. A., Schultz, D., Nadell, C. D. & Cramer, R. A. Fungal biofilm architecture produces hypoxic microenvironments that drive antifungal resistance. *Proc. Natl. Acad. Sci.* **117**, 22473–22483 (2020).
39. Wang, Q. H. et al. Integrated transcriptomics and metabolomics reveal changes in cell homeostasis and energy metabolism in *Trachinotus ovatus* in response to acute hypoxic stress. *Int. J. Mol. Sci.* **25**, 1054 (2024).
40. Martin, C. E., Oh, C. S., Kandasamy, P., Chellapa, R. & Vemula, M. Yeast desaturases. *Biochem. Soc. Trans.* **30**, 1080–1082 (2002).
41. Nakagawa, Y., Sakumoto, N., Kaneko, Y. & Harashima, S. Mga2p is a putative sensor for low temperature and oxygen to induce OLE1 transcription in *Saccharomyces cerevisiae*. *Biochem. Biophys. Res. Commun.* **291**, 707–713 (2002).
42. Gostinčar, C., Turk, M., Plemenitaš, A. & Gunde-Cimerman, N. The expressions of Δ9-, Δ12-desaturases and an elongase by the extremely halotolerant black yeast *Hortaea werneckii* are salt dependent. *FEMS Yeast Res.* **9**, 247–256 (2009).
43. Jackson, F. M. et al. Biosynthesis of C18 polyunsaturated fatty acids in microsomal membrane preparations from the filamentous fungus *Mucor circinelloides*. *Eur. J. Biochem.* **252**, 513–519 (1998).
44. He, M., Qin, C. X., Wang, X. & Ding, N. Z. Plant unsaturated fatty acids: Biosynthesis and regulation. *Front. Plant. Sci.* **11**, 390 (2020).
45. Striesow, J. et al. Hypoxia increases triacylglycerol levels and unsaturation in tomato roots. *BMC Plant Biol.* **24**, 909 (2024).
46. Xie, L. J., Zhou, Y., Chen, Q. F. & Xiao, S. New insights into the role of lipids in plant hypoxia responses. *Prog Lipid Res.* **81**, 101072 (2021).
47. Wickramarathna, A. D. et al. Heterologous expression of flax PHOSPHOLIPID:DIACYLGLYCEROL CHOLINEPHOSPHOTRANSFERASE (PDCT) increases polyunsaturated fatty acid content in yeast and Arabidopsis seeds. *BMC Biotechnol.* **15**, 63 (2015).
48. Brunkard, J. O. Exaptive evolution of target of Rapamycin signaling in multicellular eukaryotes. *Dev. Cell.* **54**, 142–155 (2020).
49. An, H., Ordureau, A., Körner, M., Paulo, J. A. & Harper, J. W. Systematic quantitative analysis of ribosome inventory during nutrient stress. *Nature* **583**, 303–309 (2020).
50. Arancibia, C., Navarro-Lisboa, R., Zúñiga, R. N. & Matiacevich, S. Application of CMC as thickener on nanoemulsions based on olive oil: Physical properties and stability. *Int. J. Polym. Sci.* **2016**, 6280581 (2016).
51. Berninger, T., Dietz, N. & González López, Ó. Water-soluble polymers in agriculture: Xanthan gum as eco-friendly alternative to synthetics. *Microb. Biotechnol.* **14**, 1881–1896 (2021).
52. Ermakova, E. A. et al. Investigation of the amount of Polyvinylpyrrolidone as gelling agent to lanthanum Cobaltite micropowders synthesized by sol-gel method. *Inorg. Mater. Appl. Res.* **14**, 1422–1428 (2023).
53. Adelin, E., Slimani, N., Cortial, S., Schmitz-Alfonso, I. & Ouazzani, J. Platotex: an innovative and fully automated device for cell growth scale-up of agar-supported solid-state fermentation. *J. Ind. Microbiol. Biotechnol.* **38**, 299–305 (2011).
54. Philipp, L. A., Bühler, K., Ulber, R. & Gescher, J. Beneficial applications of biofilms. *Nat. Rev. Microbiol.* **22**, 276–290 (2024).
55. Zhu, M., Yu, L. J., Li, W., Zhou, P. P. & Li, C. Y. Optimization of arachidonic acid production by fed-batch culture of *Mortierella alpina* based on dynamic analysis. *Enzym. Microb. Technol.* **38**, 735–740 (2006).
56. Bao, Z. et al. New insights into phenotypic heterogeneity for the distinct lipid accumulation of *Schizochytrium* sp. H016. *Biotechnol. Biofuels Bioprod.* **15**, 33 (2022).
57. Chen, W. et al. Transcriptome analysis reveals that up-regulation of the fatty acid synthase gene promotes the accumulation of docosahexaenoic acid in *Schizochytrium sp.* S056 when glycerol is used. *Algal Res.* **15**, 83–92 (2016).
58. Yin, Y. et al. Class A lysophosphatidic acid acyltransferase 2 from *Camelina sativa* promotes very long-chain fatty acids accumulation in phospholipid and triacylglycerol. *Plant. J.* **112**, 1141–1158 (2022).
59. Fisk, H. L., West, A. L., Childs, C. E., Burdge, G. C. & Calder, P. C. The use of gas chromatography to analyze compositional changes of fatty acids in rat liver tissue during pregnancy. *J. Vis. Exp.* **51445** https://doi.org/10.3791/51445 (2014).
60. Li, B. & Dewey, C. N. RSEM: accurate transcript quantification from RNA-Seq data with or without a reference genome. *BMC Bioinform.* **12**, 323 (2011).
61. Ashburner, M. et al. Gene ontology: tool for the unification of biology. *Nat. Genet.* **25**, 25–29 (2000).
62. Aleksander, S. A. et al. The gene ontology knowledgebase in 2023. *Genetics* **224**, iyad031 (2023).
63. Kanehisa, M. & Goto, S. KEGG: Kyoto encyclopedia of genes and genomes. *Nucleic Acids Res.* **28**, 27–30 (2000).
64. Kanehisa, M., Furumichi, M., Sato, Y., Matsuura, Y. & Ishiguro-Watanabe, M. KEGG: biological systems database as a model of the real world. *Nucleic Acids Res.* **53**, D672–D677 (2025).
65. Subramanian, A. et al. Gene set enrichment analysis: A knowledge-based approach for interpreting genome-wide expression profiles. *Proc. Natl. Acad. Sci.* **102**, 15545–15550 (2005).
66. Wickham, H. Data analysis. In ggplot2: Elegant Graphics for Data analysis (ed Wickham, H.). 189–201. https://doi.org/10.1007/978-3-319-24277-4_9 (Springer, 2016).

Acknowledgements

This study was financially supported by the National Natural Science Foundation of China (grant number 21908074). The qRT-PCR analysis was performed at the Research Core Facilities for Life Science, Huazhong University of Science and Technology (HUST). The authors would like to sincerely thank all those who provided support. Additionally, we express our deep gratitude to the Key Laboratory of Arable Land Conservation (Mid-

dle and Lower Reaches of Yangtze River), Ministry of Agriculture and Rural Affairs, at the College of Resources and Environment, Huazhong Agricultural University, for providing the essential equipment for this research.

Author contributions

Tingting Liu and Pandeng Li conceived the ideas, designed the research, and conducted the data collection. Tingting Liu wrote the manuscript. Pandeng Li reviewed and revised the manuscript. Ziqi Ou and Tianyi Yu conducted analysis of transcriptome data. Yumei Feng and Bohan Wang performed lipid detection. Longjiang Yu and Yuanmin Zhu supervised the research and contributed to fund acquisition. All authors read and approved the final manuscript.

Declarations

Competing interests

The authors declare no competing interests.

Additional information

Supplementary Information The online version contains supplementary material available at https://doi.org/10.1038/s41598-025-00965-9.

Correspondence and requests for materials should be addressed to Y.Z. or L.Y.

Reprints and permissions information is available at www.nature.com/reprints.

Publisher's note Springer Nature remains neutral with regard to jurisdictional claims in published maps and institutional affiliations.